

Capacity fading of spinel phase LiMn_2O_4 with cycling

Myoung Youp Song^{a,*}, Dong Su Ahn^a, Hye Ryoung Park^b

^a Division of New Materials Engineering, Automobile High-Technology Research Institute, Chonbuk National University, 664-14 Iga Deogjindong Deogjingu Chonju, Chonbuk, 561-756, South Korea

^b Division of Applied Chemical Engineering, Chonnam National University, 300 Yongbongdong Bukgu Kwangju, 500-757, South Korea

Received 11 November 1998; received in revised form 15 March 1999; accepted 16 March 1999

Abstract

The capacity fading with cycling between 3.5 V and 4.3 V of the spinel phase LiMn_2O_4 reveals the decrease in the lengths of two voltage plateaus at 4.15 V and 4.0 V in the V vs. x curves, corresponding to the two-phase reaction and the one-phase reaction, respectively. These reactions are also shown by the oxidation and reduction peaks in the cyclic voltammogram. As the number of cycle increases, the regions of the two-phase reaction and the one-phase reaction in the V vs. x curves decrease simultaneously. The lattice destruction induced by strain causes the capacity fading of LiMn_2O_4 with cycling. The expansion and contraction of spinel phase LiMn_2O_4 due to the intercalation and deintercalation make the unit cell strained and distorted. With cycling, the interstitial sites and thus the spinel structure will be destroyed. This decreases the fraction of the spinel phase, leading to the capacity fading of LiMn_2O_4 with cycling. Vacancy of interstitial sites by the deintercalation of Li ions and the attraction of oxygen with the remaining Li ions make shorter the lattice parameters of the cubic structure phases as the deintercalation proceeds. © 1999 Elsevier Science S.A. All rights reserved.

Keywords: Spinel phase LiMn_2O_4 ; Capacity fading; Cycling; Strain; Destruction of spinel phase

1. Introduction

The spinel LiMn_2O_4 is a very promising cathode material with economical and environmental advantages compared with layered compounds such as LiCoO_2 and LiNiO_2 . However, the spinel LiMn_2O_4 shows severe capacity fading with cycling as compared with LiCoO_2 . To improve the cycling performance of spinel phase LiMn_2O_4 , the quaternary spinel phases $\text{LiM}_y\text{Mn}_{2-y}\text{O}_4$ ($M = \text{Co}, \text{Cr}, \text{Ni}, \text{B}, \text{Fe}, \text{Ti}$) were studied [1,2].

In the spinel LiMn_2O_4 , Li ions occupy tetrahedral (8a) sites, Mn ions ($\text{Mn}^{3+}/\text{Mn}^{4+}$) octahedral (16d) sites, and O^{2-} ions octahedral (32e) sites [3,4]. These oxygen ions form a cubic closed-packed array. Tetrahedral (8a) sites share face with vacant octahedral sites (16c), so that they form a 3-dimensional vacant channels. Li ions can intercalate/deintercalate through these channels during the electrochemical reaction. In the spinel $\text{Li}_x\text{Mn}_2\text{O}_4$, structural transformation occurs during the electrochemical reaction. When $0 \leq x \leq 1$, $\text{Li}_x\text{Mn}_2\text{O}_4$ remains a cubic spinel structure at near 4 V. On the other hand, when $1 < x \leq 2$, phase

transition occurs from cubic symmetry to tetragonal at near 3 V [5,6]. Ohzuku et al. [5] showed that at an average composition range of $0.27 < x < 0.60$ in $\text{Li}_x\text{Mn}_2\text{O}_4$, the reduction proceeded in two cubic phases ($a_c = 8.045 \text{ \AA}$, $a_c = 8.142 \text{ \AA}$), which are characterized by voltage plateau region at 4.11 V, 3.94 V, respectively in the discharge curves, and at a composition range of $0.6 < x < 1.0$ reduction proceeded in homogeneous phase. Xia and Yoshia [7] reported that a two-phase reaction (cubic $a_0 = 8.154 \text{ \AA}$ and $a_0 = 8.072 \text{ \AA}$) occurred in the range of $0.1 < x < 0.45$, and a one-phase reaction (cubic $a_0 = 8.163 \text{ \AA}$ to 8.247 \AA) occurred in the range of $0.45 < x < 1.0$ for the first charge. At a composition range of $1 < x \leq 2$, the reduction proceeded in two phases, cubic phase ($a_c = 8.239 \text{ \AA}$) and tetragonal phase ($a_T = 5.649 \text{ \AA}$, $c_T = 9.253 \text{ \AA}$), which is characterized by voltage plateau region of discharge curve at 2.96 V. The 3 V plateau represents the intercalation of a second lithium to the spinel phase ($\text{LiMn}_2\text{O}_4 \rightarrow \text{Li}_2\text{Mn}_2\text{O}_4$), whereas the 4.1 V plateau implies the removal of one lithium to the spinel phase ($\text{LiMn}_2\text{O}_4 \rightarrow \lambda\text{-MnO}_2$) [8,9]. In this work, we studied the capacity fading with cycling of spinel phase LiMn_2O_4 as a cathode material by comparing its electrochemical properties with those of $\text{LiFe}_{0.5}\text{Mn}_{1.5}\text{O}_4$. We discussed also the decrease in the

* Corresponding author. Tel.: +82-652-270-2379; Fax: +82-652-270-2386; E-mail: songmy@moak.chonbuk.ac.kr

lattice parameters of the cubic phases as the deintercalation proceeds. Charging and discharging was carried out in a voltage range between 3.5 V and 4.3 V, where cubic spinel structure was maintained.

2. Experimental

LiMn_2O_4 sample was synthesized by solid-state reaction. Mixture of LiOH and $\text{MnO}_2(\text{CMD})$ with 1:2 molar ratio was calcined at 400°C for 10 h, and then sintered at 750°C for 48 h in air with intermediate grinding. After adding the appropriate amount of Fe_2O_3 to LiOH and MnO_2 , $\text{LiFe}_{0.5}\text{Mn}_{1.5}\text{O}_4$ was synthesized at 750°C by the above same process. The samples were slowly cooled at a cooling rate of $1^\circ\text{C}/\text{min}$. The phase identification of the prepared samples were carried out by X-ray diffraction analysis using CuK_α radiation (Mac-Science). To measure the electrochemical properties of the $\text{LiFe}_y\text{Mn}_{2-y}\text{O}_4$ ($y = 0.0$ and 0.5), the electrochemical cells consisted of a $\text{LiFe}_y\text{Mn}_{2-y}\text{O}_4$ as positive electrode, Li metal as the negative electrode, and electrolyte of 1 M LiPF_6 in a 2:1 (volume ratio) mixture of ethylene carbonate (EC) and dimethyl carbonate (DMC). A glass-filter was used as the separator. The cathodes were mixtures of 89 wt.% active material, 10 wt.% acetylene black, and 1 wt.% polytetrafluoroethylene (PTFE) binder. The cells were assembled in argon-filled dry box. All the electrochemical tests were performed at room temperature with a potentiostatic-galvanostatic system (Mac-Pile system, Bio-Logic). The electrochemical tests were conducted in a two-electrode cell. The cells were cycled between 3.5 V and 4.3 V at current density $265 \mu\text{A}/\text{cm}^2$. In the potentiodynamic system, voltage was scanned at a low rate of $10 \text{ mV}/\text{h}$.

3. Results

The X-ray diffraction (XRD) patterns of the $\text{LiFe}_y\text{Mn}_{2-y}\text{O}_4$ ($y = 0.0$ and 0.5) sintered at 750°C for 48 h

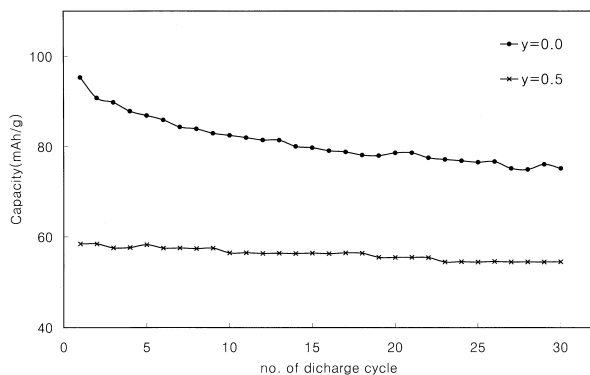


Fig. 1. Variation of discharge capacities for $\text{Li}/\text{LiFe}_y\text{Mn}_{2-y}\text{O}_4$ ($y = 0.0$ and 0.5) with the number of discharge cycle between 3.5 and 4.3 V at current density $265 \mu\text{A}/\text{cm}^2$ during 30 cycles.

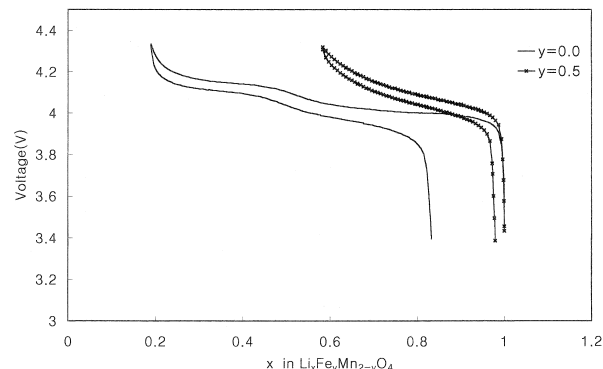


Fig. 2. The first charge and discharge curves of $\text{Li}/\text{LiFe}_y\text{Mn}_{2-y}\text{O}_4$ ($y = 0.0$ and 0.5) between 3.5 and 4.3 V at current density $265 \mu\text{A}/\text{cm}^2$.

were identified with the cubic spinel having a space group $\text{Fd}3\text{m}$. When the amount of substitution (y) was larger than 0.5 , the peaks for impurity appeared. The lattice parameters of the samples were obtained by least square method. Those of $\text{LiFe}_y\text{Mn}_{2-y}\text{O}_4$ ($y = 0.0$ and 0.5) were $a_c = 8.231 \text{ \AA}$ and 8.249 \AA , respectively.

Fig. 1 shows the variation of discharge capacities for $\text{Li}/\text{LiFe}_y\text{Mn}_{2-y}\text{O}_4$ ($y = 0.0$ and 0.5) with the number of cycle. The cells were cycled 30 times at a current density $265 \mu\text{A}/\text{cm}^2$ between 3.5 V and 4.3 V. The capacity of LiMn_2O_4 decreases very rapidly and then slowly whereas that of $\text{LiFe}_{0.5}\text{Mn}_{1.5}\text{O}_4$ decreases very slowly. The capacity losses during 30 cycles are about 21% and 7% of initial capacities for $y = 0.0$ and $y = 0.5$, respectively.

Fig. 2 shows the variation of lithium-ion concentration (x) with voltage (V) of $\text{Li}/\text{LiFe}_y\text{Mn}_{2-y}\text{O}_4$ ($y = 0.0$ and 0.5) for the first cycle in a voltage range 3.5 V–4.3 V at constant current density $265 \mu\text{A}/\text{cm}^2$. For $\text{Li}_x\text{Mn}_2\text{O}_4$ ($y = 0.0$) two plateau voltages are observed at 4.0 V and 4.15 V. It is considered that two plateau voltages observed in Fig. 2 correspond to a two-phase reaction and a one-phase reaction, respectively. For $\text{Li}_x\text{Fe}_{0.5}\text{Mn}_{1.5}\text{O}_4$ an ambiguous plateau appears in the V vs. x curve.

Fig. 3 shows the cyclic voltammograms of $\text{Li}/\text{LiFe}_y\text{Mn}_{2-y}\text{O}_4$ ($y = 0.0$ and 0.5) in the voltage range

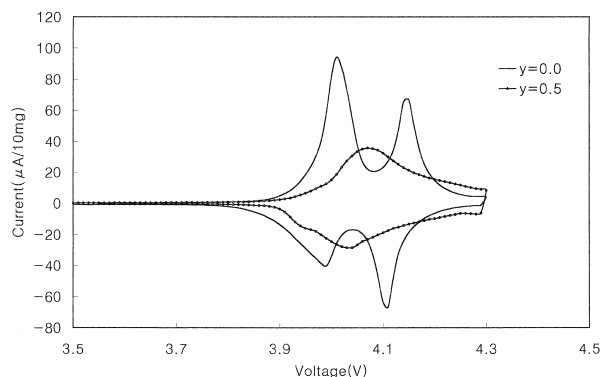


Fig. 3. The cyclic voltammograms of $\text{Li}/\text{LiFe}_y\text{Mn}_{2-y}\text{O}_4$ ($y = 0.0$ and 0.5) between 3.5 and 4.3 V at scan rate $10 \text{ mV}/\text{h}$.

3.5–4.3 V. For LiMn_2O_4 , the oxidation and reduction peaks are located near 4.01 and 4.15 V, 4.11 and 3.99 V, respectively, showing that oxidation and reduction proceed in two stages. The voltages for the oxidation peaks of $\text{Li}_x\text{Mn}_2\text{O}_4$ agree well to the two plateau voltages of the V vs. x curve for $\text{Li}_x\text{Mn}_2\text{O}_4$ in Fig. 2. For $\text{LiFe}_{0.5}\text{Mn}_{1.5}\text{O}_4$, the second peaks for oxidation and reduction processes respectively do not appear distinctly.

Fig. 4 shows the charge–discharge curves of (a) $\text{Li}/\text{Li}_x\text{Mn}_2\text{O}_4$ and (b) $\text{Li}/\text{Li}_x\text{Fe}_{0.5}\text{Mn}_{1.5}\text{O}_4$ cells in a voltage range 3.5 V–4.3 V at constant current density $265 \mu\text{A}/\text{cm}^2$. In Fig. 4(a), for $\text{Li}/\text{Li}_x\text{Mn}_2\text{O}_4$ cell, two voltage plateaus in the V vs. x curves are observed. As the number of cycle increases, the lengths of two plateaus decrease, indicating the regions of the two-phase reaction and the one-phase reaction decrease simultaneously. This suggests that the fraction of the spinel phase LiMn_2O_4 decreases with cycling. This observation is different from that of Xia and Yoshia [7], who reported that capacity loss occurs only on the higher voltage plateau. In Fig. 4(b), for $\text{Li}/\text{Li}_x\text{Fe}_{0.5}\text{Mn}_{1.5}\text{O}_4$ cell, one voltage plateau in the V vs. x curves is observed.

Figs. 2–4 show that charging and discharging involves two stages (a two-phase reaction and a one-phase reaction) for LiMn_2O_4 , and one stage (a one-phase reaction) for $\text{LiFe}_{0.5}\text{Mn}_{1.5}\text{O}_4$.

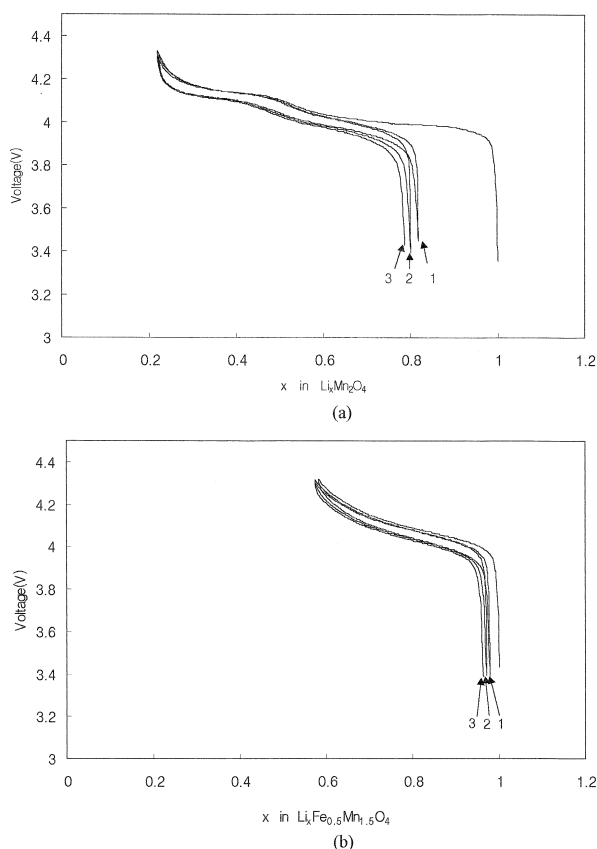


Fig. 4. Charge–discharge curves of $\text{Li}/\text{LiFe}_y\text{Mn}_{2-y}\text{O}_4$ cells as a function of x ; (a) $y = 0.0$ and (b) $y = 0.5$.

All the above results show that LiMn_2O_4 , involving two stages in charging and discharging, has a larger initial capacity but exhibits capacity fading with cycling. $\text{LiFe}_{0.5}\text{Mn}_{1.5}\text{O}_4$, involving one stage in charging and discharging, has a smaller initial capacity but exhibit slower capacity fading with cycling, as compared with LiMn_2O_4 .

4. Discussion

In Fig. 4(a), we can see that, as compared with the quantity of the deintercalated Li ions by the first charging, that of the intercalated Li ions by the first discharging is much smaller. It is considered that it is because, during the first charging, Li ions not only deintercalate from tetrahedral (8a) sites but also come out from Li atoms which may be contained in excess outside the tetrahedral (8a) sites within the sample. The quantity of Li ions which come from the Li atoms outside the tetrahedral (8a) sites for the following charging will become much smaller as the number of cycle increases. In Fig. 4(b), we can see that, the difference between the quantity of the deintercalated Li ions and that of the intercalated Li ions for the first cycle is relatively small as compared with $\text{Li}/\text{Li}_x\text{Mn}_2\text{O}_4$ cell. This shows that, for the first charging, most of the deintercalated Li ions come from the tetrahedral (8a) sites of the spinel structure, and that a few Li ions come from the Li atoms which does not form the spinel structure.

Ohzuku et al. [5] and Xia and Yoshio [7] reported that the lattice parameters of the cubic phases decreased as the value x in $\text{Li}_x\text{Mn}_2\text{O}_4$ decreases at near 4 V.

The range of the value x in deintercalation and intercalation is $\sim 0.21 \leq x \leq \sim 0.81$ for $\text{Li}_x\text{Mn}_2\text{O}_4$ and $\sim 0.58 \leq x \leq \sim 0.98$ for $\text{Li}_x\text{Fe}_{0.5}\text{Mn}_{1.5}\text{O}_4$. Thus, the quantities of the reversible Li ions are about $0.6 \text{ Li}^+/\text{mol}$ and $0.4 \text{ Li}^+/\text{mol}$. The wider range of the value of x in LiMn_2O_4 than in $\text{LiFe}_{0.5}\text{Mn}_{1.5}\text{O}_4$ is related to the more rapid fading of capacity of LiMn_2O_4 with cycling. The larger expansion and contraction in the lattice parameter due to the intercalation and deintercalation over the larger range of the value x in $\text{Li}_x\text{Mn}_2\text{O}_4$ will make the unit cell more strained as compared with $\text{LiFe}_{0.5}\text{Mn}_{1.5}\text{O}_4$. This will distort more the interstitial sites of $\text{Li}_x\text{Mn}_2\text{O}_4$. With cycling, the interstitial site and thus the spinel structure of $\text{Li}_x\text{Mn}_2\text{O}_4$ will be more destroyed, leading to the further decrease in the quantity of the spinel phase, as compared with $\text{LiFe}_{0.5}\text{Mn}_{1.5}\text{O}_4$. This results in more rapid fading of capacity LiMn_2O_4 with cycling, as compared with $\text{LiFe}_{0.5}\text{Mn}_{1.5}\text{O}_4$. This is reflected as the difference of the slopes in the capacity–cycle curves in Fig. 1.

In summary, the lattice destruction induced by strain causes the capacity fading of LiMn_2O_4 with cycling. The expansion and contraction of spinel phase LiMn_2O_4 due to the intercalation and deintercalation make the unit cell strained and distorted. With cycling, the interstitial sites and thus the spinel structure will be destroyed. This de-

creases the fraction of the spinel phase, leading to the capacity fading of LiMn_2O_4 with cycling.

The lattice parameters of the cubic phases decreased as the deintercalation proceeded at near 4 V, as mentioned above. As Li ions deintercalates, the number of positive Li ions becomes smaller. Vacancy of interstitial sites by the deintercalation will make the unit cell smaller, and the attractive force of oxygen, the quantity of which remains constant, with the remaining Li ions will become stronger, also decreasing the size of the unit cell as the deintercalation of Li ions proceeds.

5. Conclusions

The capacity fading of the spinel phase LiMn_2O_4 with cycling between 3.5 V and 4.3 V reveals the decreases in the lengths of two voltage plateaus at 4.15 V and 4.0 V, corresponding to the two-phase reaction and the one-phase reaction, respectively. These reactions are also shown by the oxidation and reduction peaks in the cyclic voltammogram. As the number of cycle increases, the regions of the two-phase reaction and the one-phase reaction in the V vs. x curves decrease simultaneously.

The lattice destruction induced by strain causes the capacity fading of LiMn_2O_4 with cycling. The expansion and contraction of spinel phase LiMn_2O_4 due to the intercalation and deintercalation make the unit cell strained and distorted. With cycling, the interstitial sites and thus the spinel structure will be destroyed. This decreases the frac-

tion of the spinel phase, leading to the capacity fading of LiMn_2O_4 with cycling.

Vacancy of interstitial sites by the intercalation of Li ions and the attraction of oxygen with the remaining Li ions make shorter the lattice parameters of the cubic structure phase as the deintercalation proceeds.

Acknowledgements

The partial financial support of Automobile High-Technology Research Institute at Chonbuk National University is gratefully acknowledged.

References

- [1] L. Guohua, H. Ikuta, T. Uchida, M. Wakihara, J. Electrochem. Soc. 143 (1996) 178.
- [2] A.D. Robertson, S.H. Lu, W.F. Averill, W.F. Howard Jr., J. Electrochem. Soc. 144 (1997) 3500.
- [3] M.M. Thackeray, W.I.F. David, P.G. Bruce, J.B. Goodenough, Mater. Res. Bull. 18 (1983) 461.
- [4] M.M. Thackeray, P.J. Johnson, L.A. de Picciotto, Mater. Res. Bull. 19 (1984) 179.
- [5] T. Ohzuku, M. Kitagawa, T. Hirai, J. Electrochem. Soc. 137 (1990) 769.
- [6] M.M. Thackeray A de Kock, M.H. Rossouw, D. Liles, R. Bittihn, D. Hoge, J. Electrochem. Soc. 139 (1992) 363.
- [7] Y. Xia, M. Yoshia, J. Electrochem. Soc. 143 (1996) 825.
- [8] J.M. Tarascon, E. Wang, F.K. Shokoohi, W.R. Mckinnon, S. Colson, J. Electrochem. Soc. 138 (1991) 2859.
- [9] G. Pistoia, Solid State Ionics 58 (1992) 285.